SART-Res-UNet: Fan Beam CT Image Reconstruction from Limited Projections using attention-enabled residual U-Net

Harika Jinka HARIKAJINKA@GMAIL.COM
Jyothsna Shaji JYOTHSNASHAJI99@GMAIL.COM
Sangeeth John SANGEETHJOHN1997@GMAIL.COM
Sreeraj R Menon SREERAJMENON98@GMAIL.COM
Amalu Pradeep AMALUPRADEEPT@GMAIL.COM
Jayaraj P B JAYARAJPB@NITC.AC.IN
Pournami P N POURNAMIPN@NITC.AC.IN
Department of Computer Science and Engineering, National Institute of Technology Calicut, Pin 673 601, Kerala, India

Niyas Puzhakkal NIYAS.PUZHAKKAL@MVRCCRI.CO
MVR Cancer Center and Research Institute, Calicut, Kerala, India

Editors: Berrin Yanıkoğlu and Wray Buntine

Abstract

CT scans significantly improve analytical competencies but uses X-Rays which will produce ionizing radiation that bring higher radiation to the living tissues. Thus, optimization of CT radiation dose has a significant concern to lower the health risks. Many manufacturers have done a greater contribution by developing technologies to reduce dosage by maintaining image quality by adding noise reduction filters, automatic exposure control, and using many iterative reconstruction algorithms. Image reconstruction algorithms play a vital role in maintaining or improving image quality in reduced-dose CT. The present research work combines the state-of-the-art reconstruction technique Simultaneous Algebraic Reconstruction Technique (SART) with a Residual U-Net network to generate images from limited number of sinograms. The proposed model is trained using sinograms corresponding head and neck and head CT images of 10 patients. The proposed model predicted superior diagnostic quality images with max PSNR of 70.23 and Structural Similarity Index Measure (SSIM) of 0.99. Thus the proposed model, *SART-Res-Unet*, ensures a very low radiation exposure to a patient during the repeated CT imaging sequence, which is an inevitable part of radiotherapy.

Keywords: CT; Image Reconstruction; U-Net; Sparse Reconstruction; deep learning

1. Introduction

Computed tomography is an imaging procedure that uses rotating X-ray machines and computers to create cross-sectional images of human body. The images produced by this reconstruction are more comprehensive than X-Ray images Lifeng YuXin Liu and Ramirez-Giraldo (2017). They give a wide-ranging view of soft tissues, blood vessels, and bones in various parts of the body. The image slices can also be stacked together to produce a 3D image of any anatomical area of the human body. Medical experts use CT images to diagnose hemorrhages, joint fractures, tumors, and blood clots. CT scanner has a pivoting

X-beam source that discharges limited X-ray beams that pass through the patient. The discharging beams are then verified and recorded by identifiers. Finally, image reconstruction algorithms are employed to generate the CT image Cynthia H. McCollough (2017).

Nowadays there is a significant increase in the use of CT. In any case, it works on a higher radiation portion than ordinary indicative x-rays. The radio-sensitive tissues are chiefly situated inside the fringe vision of typical chest, stomach, and pelvic regions. A typical stomach assessment portion is in the range of 10mSv and 20mSv Lifeng YuXin Liu and Ramirez-Giraldo (2017) while bosom glandular portion is 20mSv during a pneumonic course CT angiogram. Most patients are exposed to various assessments over the span of their treatment which expands the aggregate dose. Exposing to ionizing radiation is disrupting due to its harmful nature to healthy living tissues. Radiation exposure can be brought down to greater extent by restricted scanning. Nonetheless, this results in noise generation and subsequent image distortion.

Filtered Back Projection (FBP) is the traditional methodology used for CT image generation, but it relies on having the complete projection data. It is highly desirable to generate admirable quality images with limited projection data available. To achieve this, the Simultaneous Algebraic Reconstruction Technique (SART) Shailendra Tiwari (2017) can used. SART generates images of desired quality and thus can reconstruct images that can further be enriched by passing to a suitable feature preserving technique such as deep learning.

2. Related Works

Limited angled scanning has been of interest for a long time because it is rapid and safer compared to the other conventional methods. Sidky et al. Sidky et al. (2009) proposed iterative methods that curtails the error in the image for under-sampled projection data. Jianhua et al. Luo et al. (2012) attempts to convert the ill-posed sparse reconstruction scenario into a well-defined one based on the S-transform. Researchers were also interested in compressed sensing approaches or other sparsity-inducing penalties under a data fidelity term. Such regularization methods were, however, computationally expensive.

As deep learning approaches gained popularity, Kang et al. Kan et al. (2016) was a pioneer in testing deep convolutional neural networks for low dose CTs and to show that directional wavelets incorporated with deep CNN has potent in suppressing noise. Han et al. Han et al. (2016) analyzed the advantages of residual learning in sparse CTs and shows that the multiscale U-net stands out as the most effective. Jin et al. Jin et al. (2016) proposed FBPConvNet where they demonstrated the performance of a combination of FBP and CNN in limited-angle reconstruction for parallel beam X-ray Computed Tomography. Hu Chen et al. Chen et al. (2017) cascaded an autoencoder and deconvolution network with skip connections into the residual encoder-decoder CNN with impressible results. The numerous works focusing on U-Net like architectures are backed by the fact that the streak artifacts are non uniformly distributed. Thus CNN with its wide receptive field are apt in capturing the essential feature maps.

Analytical methods have been repeatedly proved to be incapable of sparse reconstruction. Iterative method such as SART is in frontier in low dose CT as theorized by Wang et al. Wang et al. (2020). The definitive merging of SART and U-Net that they have demonstrated are noteworthy. The reconstruction of images from projections has been an

active area of research owing to its indispensable contribution to accurate medical diagnosis. However, the radiation exposure that a patient has to go through regularly could lead to terminal illnesses. The radiation dosage can be kept at a minimum by limiting the number of projections taken while scanning. In low-dose Computed Tomography, extreme artifacts usually come about due to photon starvation, beam hardening, etc., which degrade the diagnosis's reliability. As the number of angles considered decreases, the image becomes more distorted. Therefore, it is of interest to build a sophisticated method that can retain the image's quality in low-dose CT. The method we put forward incorporated attention gates that could urge the network to fixate on relevant features in the image. To the best of our knowledge this the first of the kind experiments in incorporating attention gates to U-Net for image reconstruction in low dose CT.

3. Materials and Methods

3.1. Datasets

The dataset has been collected from MVR Cancer Center and Research Institute, Calicut, Kerala, India. The dataset contains sinograms corresponding to CT scans of different anatomical areas of 10 patients. The corresponding CT images in DICOM format are also collected as ground truth to validate the proposed model. These are the de-identified CT images with no patient specific details. The input to the proposed model is a set of sinograms from limited-angle projections of the organ under consideration. The CT scans have resolutions of 512×512 pixels with varying pixel spacing and slice thicknesses between 1.25-5 mm. The model is trained separately for each organ since the number of training, validation, and testing samples vary depending on the annotations available in the CT scan. Also, the CT scans with more than 20 slices in the ground truth for the required organ only are considered in the study. Training, validation, and testing data split is in the ratio of 70:10:20 for all the organs. Sample input sinograms are given in Fig 1 and the output is the reconstructed image of higher quality.

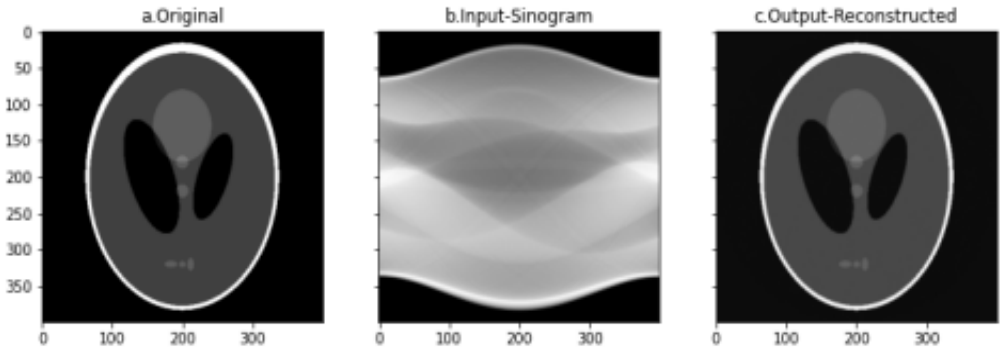

Figure 1: Input and Output images

3.2. Background

Image reconstruction in CT can be represented as an ill-posed problem as given in equation (1).

$$Ax = b \tag{1}$$

where A is the CT imaging matrix, which has $M * N$ elements.

CT image reconstruction is to acquire the unknown variable x from the known imaging grid A, and the projection information b which is accessible using the equation (1). Here, $x = (x_1, x_2, ..., x_N)^T$ and $b = (b_1, b_2, ..., b_M)^T$, which address the coefficients of discrete reconstructed image and the projection information gathered by the X-ray detectors. Fourier slice theorem, the conventional technique for image reconstruction is done using back-projection. Filtered Back-projection is the most famous algorithm utilizes the Fourier slice theorem for image reconstruction G. Wang and Fessler (2018). In any case, FBP accepts that the complete projection information is available in order to perfectly recontsruct the image.

3.3. Fan beam vs Cone beam CT imaging

Fan-beam CT (FBCT) scanner is a traditional CT that emanates a fan type X-ray beam and is identified by a linear detector array. Fan-beam scanners utilize a bended locator surface and turn around the subject's body on different occasions, obtaining X-ray line projections in the full 360° range whereas Cone-beam CT (CBCT) scanner emanates a cone type X-ray beam which is detected by flat plated sensor. Research shows that fan beam CT produces high resolution images than that of cone beam CT frameworks. A schematic representation of the image formation in FBCT and CBCT Yavuz et al. (2017) is given in Figure 2.

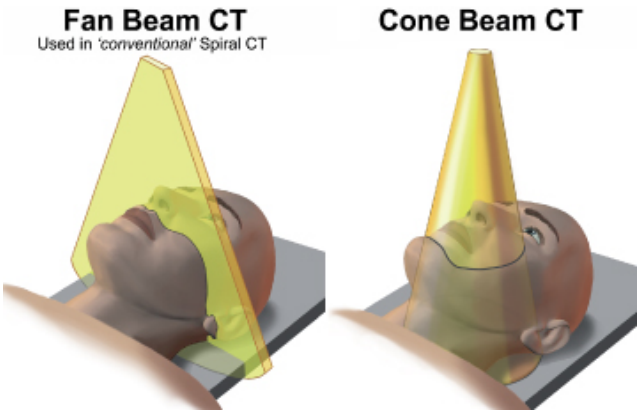

Figure 2: Fan beam and Cone beam scanning procedure

In radiotherapy, CBCT is primarily used for accurate patient positioning and FBCT is employed for treatment planning for real radiation delivery.

3.4. Simultaneous Algebraic Reconstruction Technique (SART)

Simultaneous Algebraic Reconstruction Technique (SART) Shailendra Tiwari (2017) is an iterative strategy with a benefit of applying error correction for beams in a projection simultaneously with the image reconstruction process instead of the conventional sequential image back-projection pattern. This altogether lessens the noise and thus is a better approach. Iterative update in the SART technique is represented as given in equation (2).

$$f_j^{(n+1)} = f_j^{(n)} + \beta \frac{1}{a_+ j} \sum_{i=1}^{M} \frac{a_i j}{a_i +} (b_i - A_i f^{(n)}) \tag{2}$$

where n is the number of iterations, β is the relaxing factor. At this point, $b_i - A_i f^{(n)}$ is the difference between the actual projection data and the simulated projection data. As the iterations increase, $(b_i - A_i f^{(n)}) \to 0$ and $f^{(n)} \to f^*$, where f^* is the label image.

Down-factor states the number of divisions to be made from 0 to 360 degrees before generating the sinograms (line projections). If down-factor is 3, then angle of projections will be divided into 3 parts which is [0, 180, 360]. Similarly for down-factor 5, the angle of projections will be [0, 90, 180, 270, 360]. As down-factor increases, the number of projections will be increased. So, for limited angled tomography, the number of projections should be reduced which in turn says that down-factor should be reduced.

3.5. U-Net

U-Net Ronneberger et al. (2015) is the state of art architecture that was initially used for image segmentation. It predicts a class for each pixel. Recent works have expanded the application of U-Net in several fields. It has a wide field of view which aids it in capturing local and global features in an image. Attention gates consolidated into U-Net can highlight reactions in irrelevant image backgrounds while zeroing in on the salient components of the image. The scaling of the input image with the attention units gives prominence to the required region of interest (ROI) of the image.

U-Net has a symmetric design, comprising of two significant parts – the contracting path and the expansive path. The contracting path puts together broad convolutional process i.e., notices the standard design of convolutional network. The broad way is comprises of modified 2D Convolutional layers. U-Net utilizes numerous featured maps at each layer which expands the expressive power of network. The contracting way sticks to the ordinary plan of a convolutional network. It incorporates the consecutive usage of two 3x3 convolutions without padding, extremely one of which followed by a Rectified Linear unit(ReLU) Olaf Ronneberger (2015) activation and a 2x2 max pooling layer for down-sampling. A skip association is added between the levels which reduces the information loss due to downsampling and thus speeds up the feature learning process.

3.6. Residual U-Net

ResU-Net coordinates residual modules and attention gates with a primitive U-Net design, where a stream of gate units are added into the skip connection for featuring notable elements while disambiguating non-relative and noisy features. ResU-Net not just concentrates

plentiful semantic data to enhance the capacity of component learning, yet additionally focuses on the extensive details in the scanned images. The hierarchical network consists of three cascaded convolution layer at each level followed by non-linear activation. Batch normalization and Parametric ReLU as activation function are applied after every convolution to relieve the inward covariate shift as depicted in Fig 3. The resultant image is down-sampled by max-pooling channels of dimension 2x2 with padding. The number of filters is multiplied at each level beginning from 32 to 1024. The model will be tested with the regularization method as L_1 standardization, L_2 standardization, and Dropout. Adding a dropout of 0.5 at each level helps avoiding overfitting.

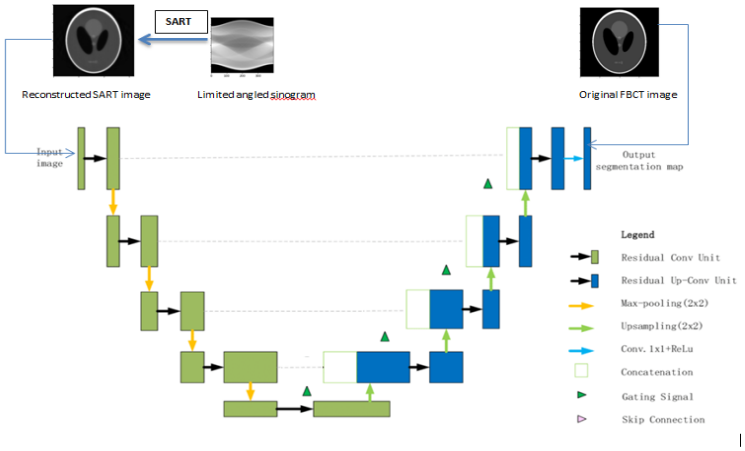

Figure 3: Residual U-Net architecture

The residual block in the architecture helps to learn deeper learning networks whereas the attention gates are consolidated during skip connections to highlight salient features that are gone through the skip connections But the time taken for training the ResU-Net is more because of multiple parameters are considered to train and segment the sparse reconstructed image prominently. The attention gate goes before the concatenation operation to guarantee that appropriate activations are merged.

The attention gate works as follows: Convolutions are applied to the image after of upsampling and the corresponding output from the contracting layer. Later, these convolution results are then added together and a non-linear activation applied. This is trailed by another convolution layer and sigmoid activation. The initial layer which is obtained from the below layer is then multiplied with the resultant filter. The gradients originated from the background are down-weighted during the backpropagation. This makes the model parameters in shallower layers to be updated primarily based on spatial regions that are critical to a given task.

Radiation dosage of CT scan can be lowered by limited scanning. However, this results in image distortion and noise. To reconstruct the high-quality image, we need to develop image reconstruction algorithms combining highly efficient feature extraction techniques with limited angle projection data. Image reconstruction generally affects the quality of images and thus on radiation portion. For a given radiation dosage, it is desirable to reproduce images with the most minimal conceivable commotion without sacrificing image

precision and spatial resolution. Reconstructions that further develop image quality can be converted into a decrease of radiation portion since images of a similar quality can be reconstructed at a lower dosage.

In the present work, we propose a hybrid architecture, for CBCT image reconstruction from limited number of X-ray projections. The first module is based on SART, which generates an image from limited angle projections. The second module is a U-net with residual units, which produces a superior quality CBCT image from the output of the first module. Hence, the low quality CBCT image is enhanced so that it can achieve a comparable diagnostic quality with the corresponding FBCT image.

3.7. Proposed SARTU-net model

The primary aim of the current research work is to develop a deep learning model which can reconstruct FBCT images of diagnostic quality from limited angle projections (sinograms). Workflow diagram of the propsoed model is given in Fig 4.

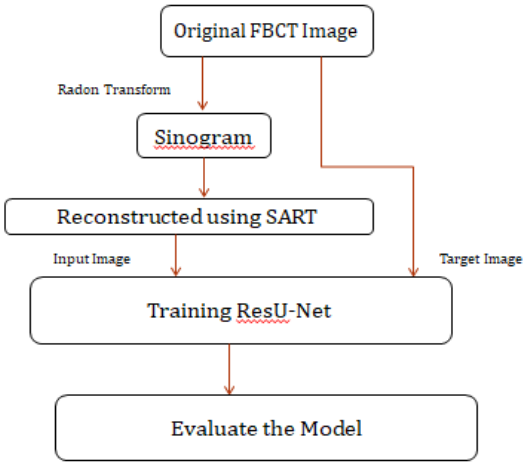

Figure 4: Workflow diagram of the proposed model

Initially, line projections (sinograms) from FBCT images are taken with a down-factor 80. This limited angled sinusoidal projection data is given as input to SART method to generate sparse reconstructed images. Now, these reconstructed images are used to train the ResU-Net architecture for generating superior quality images. The attention gate in ResU-Net highlights the salient features and reduces the irrelevant and noisy feature responses of FBCT images for better image reconstruction.

3.8. Evaluation Metrics

Root Mean Square Error (RMSE)

RMSE measures the average squared difference between the input and ground truth images. Ideally, the error should be minimum. The MSE between two images X and Y is given by equation (3).

$$MSE(X,Y) = \frac{\sum_{i=1}^{D}(X_i - Y_i)^2}{N} \tag{3}$$

where X_i and Y_i are the pixel intensities and N is the total number number of pixels.

Peak Signal Noise Ratio (PSNR)

PSNR estimates the quality of the images as given in equation (4).

$$PSNR(X,Y) = \frac{10\log_{10}(\max(\max(X),\max(Y)))^2}{X - Y^2} \tag{4}$$

where X is the reconstructed image, Y is the ground truth image.

Structural Similarity Index (SSIM)

SSIM is used to measure the structural similarity between the reconstructed image and the label image, is defined as in equation (5).

$$SSIM(X,Y) = \frac{(2\mu_Y\mu_Y + C_1) + (2\sigma_{XY} + C_2)}{(\mu_X^2 + \mu_Y^2 + C_1)(\sigma_X^2 + \sigma_Y^2 + C_2)} \tag{5}$$

where X and Y are the mean intensity values and σ_X, σ_Y denote the standard deviations, and σ_{XY} is the covariance. As the training proceeds, the images tend to become similar and thus the SSIM value tends to become 1.

4. Results and Discussion

The experiment was conducted on Google Colab which provides a single-core hyperthreaded Xeon Processor at 2.2Ghz. It provides a RAM of 12GB and Disk space of 64GB. The training was done with the help of a GPU which comes with Colab and GPU resource provided. The GPU of Colab has a Tesla K80 graphics card consisting of 2496 CUDA cores and a 12GB GDDR5 VRAM. The GPU from resource provided has 64GB GDDR5 VRAM. The proposed network was built on Tensorflow v2.

The proposed technique has precisely two phases:

- Phase 1, to generate the sparse reconstructed images from sinogram using limited angle projection data, employing SART.
- Phase 2, to increase image resolution of these generated low quality sparse images, a Res-Unet model is built and trained.

Increase in downfactor can generate good quality images from sinograms which means large amount of radiation exposure. But the main purpose of the proposed methodology is to reduce the exposure to radiation. Figure 5 shows the results CT images of different downfactors. The figure 5 represents sparse reconstructed images from sinograms with downfactor 40, 80, 150 using SART algorithm. The images with downfactor 40 will have lower quality images when compared to that of images with downfactor 150. Downfactor represents the angle at which sinograms are created and in turn sparse reconstructed images.

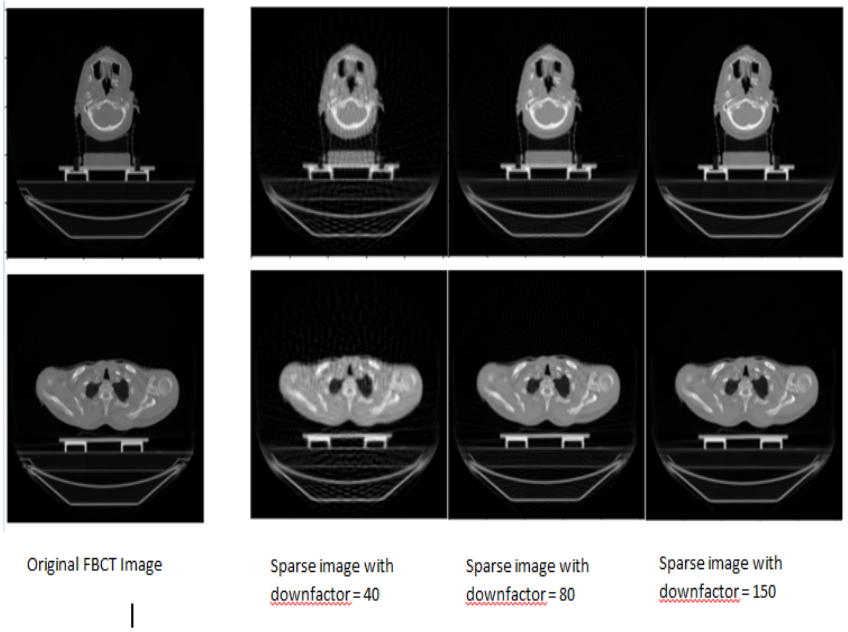

Figure 5: The reconstructed results of head and chest images comparing with original CT images at downfactor of 40, 80, 150 respectively

Patient ID	MSE	PSNR	SSIM
Patient 1	0.000796	37.01	0.688
Patient 2	0.000797	37.02	0.656
Patient 3	0.000842	36.79	0.637
Patient 4	0.000811	36.95	0.700
Patient 5	0.000795	37.02	0.714
Patient 6	0.000795	37.02	0.733
Patient 7	0.000803	37.00	0.694
Patient 8	0.000798	37.01	0.689
Patient 9	0.000797	37.02	0.676
Patient 10	0.000797	37.01	0.648

Table 1: Evaluation metric results after the SART algorithm

Time taken to sparsely reconstruct 1 patient datset is around 1 hour for a downfactor of 80. If the downfactor is increased, time taken to generate results will be increased as well but in turn increase the quality of images.

Evaluation metrics MSE, PSNR and SSIM are calculated for these images after SART algorithm is computed as reported in Table. 4. Higher the SSIM and PSNR values, greater the image resolution matches with original images.

Sparse images generated from the datasets of 10 patients with downfactor 80 are taken as feasible images for the 2nd phase. To increase this image resolution, we train a ResNet

model by dividing the given dataset as training, validation and testing. The proposed SART-Res-Unet is trained for 40 epochs. Figure 6 represents the graph of PSNR and SSIM values of training data.

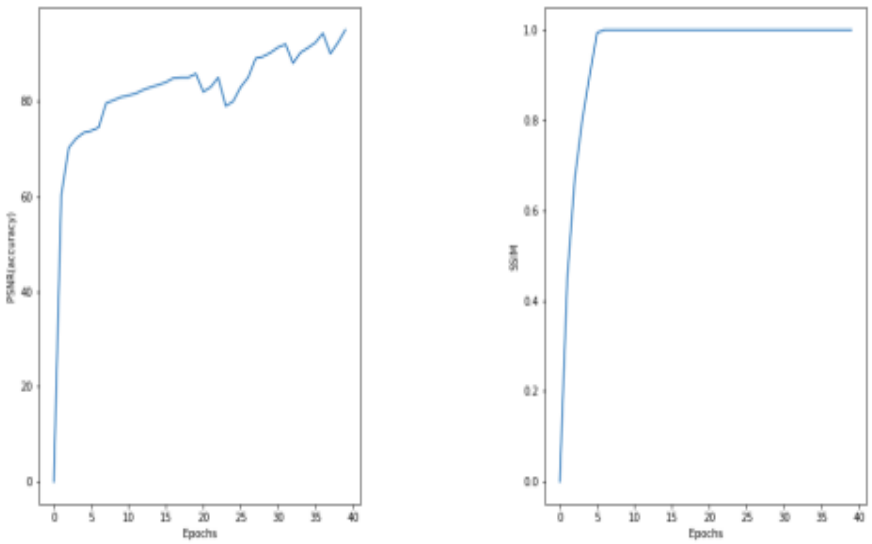

Figure 6: a) PSNR b) SSIM

MSE and PSNR values during the training and validation phases are shown in Fig. 7.

The predicted DICOM images are giving the psnr accuracy till 69.5 for downfactor 80 which is almost double the psnr value of the low quality sparse images that are reconstructed using SART algorithm. Figure 8 shows the difference of predicted CT scan image from original image and the sparse image.

Figure 9 is the predicted results for downfactor 40 which gives the psnr value till 44. As the number of projections are reduced to 40, resultant predicted image may not have the quality as good as that of Figure 8.

The random sparse reconstructed images are taken and tested to generate the resultant DICOM images to increase the quality of the image. PSNR value is calculated for the test data and plotted the graph. Increase in quality of image will increase the PSNR value. Table 4 and Table 4 shows the evalution metrics PSNR and SSIM. These tables are estimated from random prediction results for number of projections of 80 and 40. In Table 4, the maximum PSNR value is 70.2302 and the maximum SSIM is 0.9991 which is almost double the PSNR value estimated before CNN model. Similarly, the Table 4 has the PSNR value of 44.5063 and SSIM value of 0.7876.

Figure 10, is showing the quality of image before training the Residual U-Net Model which ranges from 26 to 27 for downfactor 40. After training the CNN model, the PSNR of the image has been increased to 44 as described in Table 4 which is almost double of sparse reconstructed image.

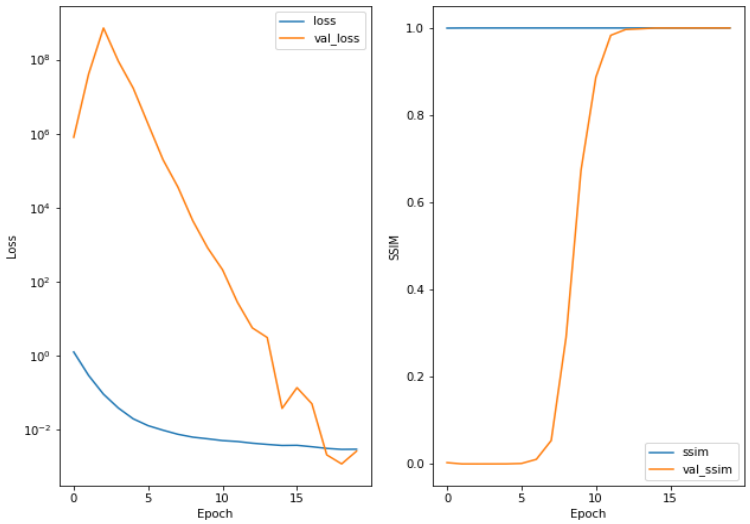

Figure 7: a)MSE b) SSIM of training and validation data

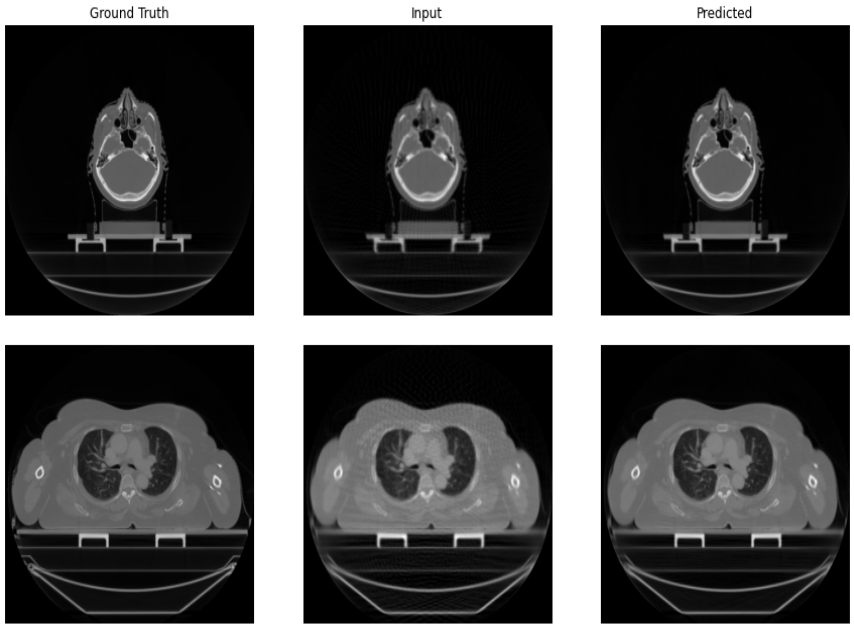

Figure 8: a)Ground Truth b) Input c) Predicted images of head and chest CT scans for downfactor 80

Figure 11 represents the graph of difference between final predicted values and the low quality DICOM image values for a downfactor of 80. Green line says the predicted data

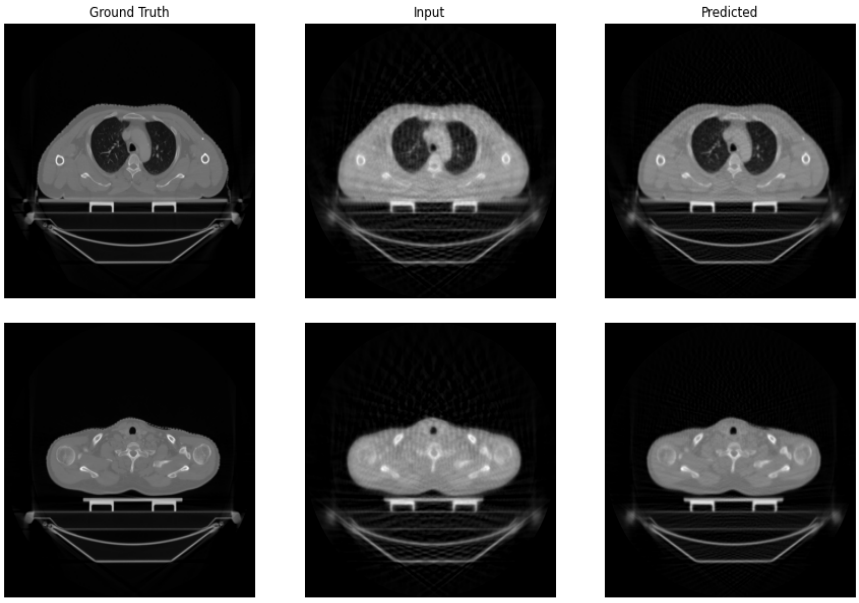

Figure 9: a)Ground Truth b) Input c) Predicted images of chest CT scans for downfactor 40

PSNR	SSIM
67.0134	0.9954
70.2302	0.9923
69.2678	0.9912
61.1295	0.9945
62.1233	0.9987
65.9876	0.9965
61.8912	0.9912
62.3535	0.9899
67.7324	**0.9991**
64.9873	0.9901

Table 2: Downfactor of 80

PSNR	SSIM
40.7989	0.7098
40.1362	0.7123
44.5063	0.7234
42.1568	0.7398
42.6461	0.703
41.7341	0.7304
41.6973	0.7656
42.0681	**0.7876**
43.8478	0.7273
40.4101	0.7176

Table 3: Downfactor of 40

PSNR values are ranging from 60 to 69.5 for the tested images and blue line are the values before training and testing the data with Residual U-Net Architecture.

When the angle of projections are reduced to 40, the psnr value will be reduced because of image quality. As the Figure 12 shows the difference in accuracy for the images before and after the CNN model for projection angles as 40.

Fig. 13 and Fig. 14 are about the zoomed CT image which shows the quality of image after training the ResU-net model for downfactor 80 and downfactor 40 respectively. The

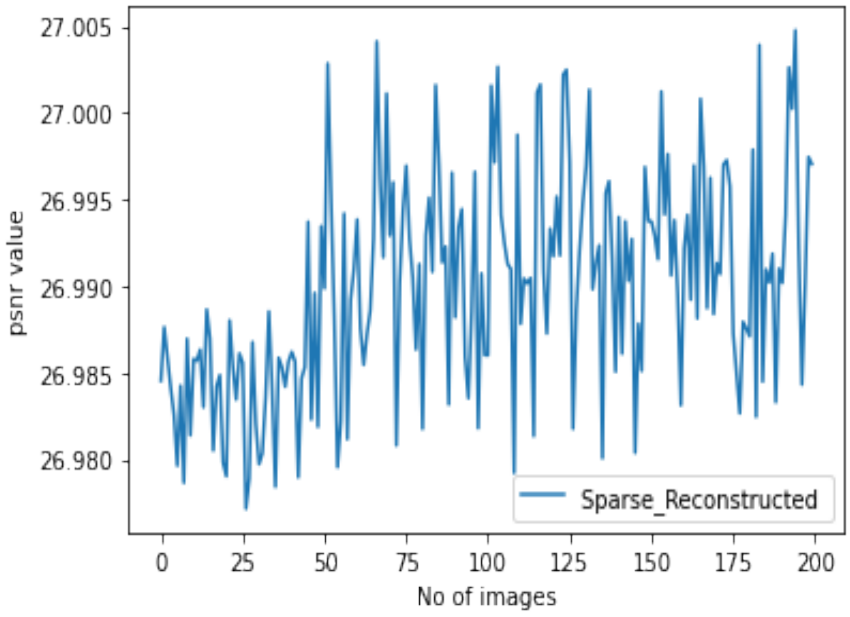

Figure 10: PSNR of Predicted and Sparse Reconstructed images for downfactor 80

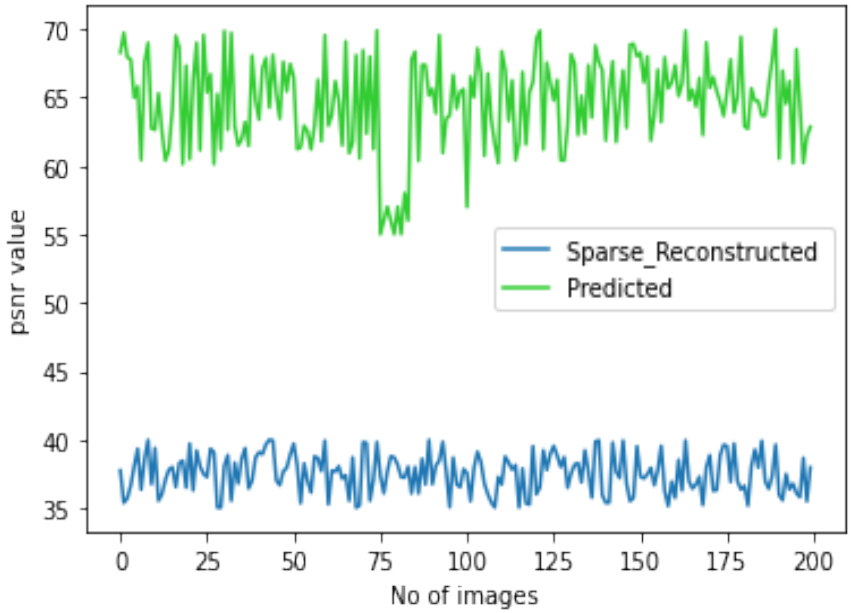

Figure 11: PSNR Graph of Predicted and Sparse Reconstructed images for downfactor 80

comparison of input image and predicted image is depicted based on ground truth. The quality of the predicted image is highly increased which is almost near to the ground truth.

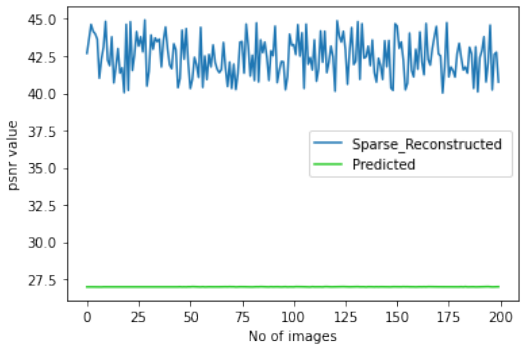

Figure 12: PSNR Graph of Predicted and Sparse Reconstructed images for downfactor 40

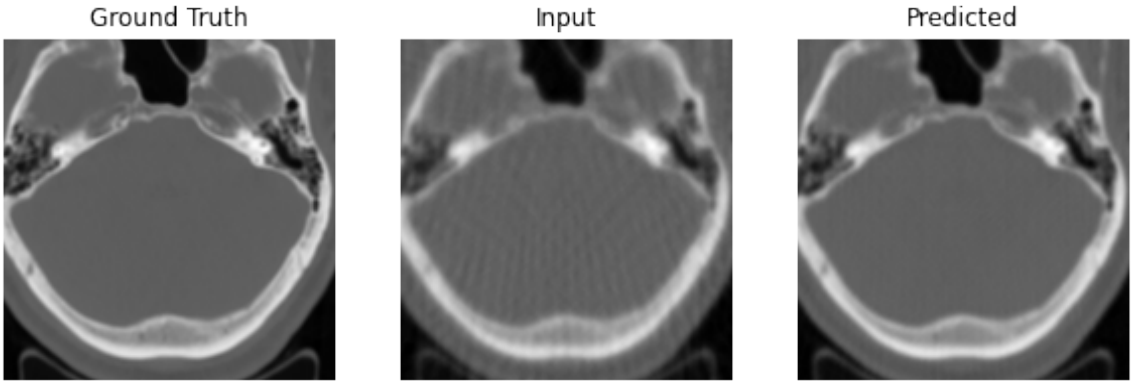

Figure 13: Zoom-In CT image of head section for downfactor 80

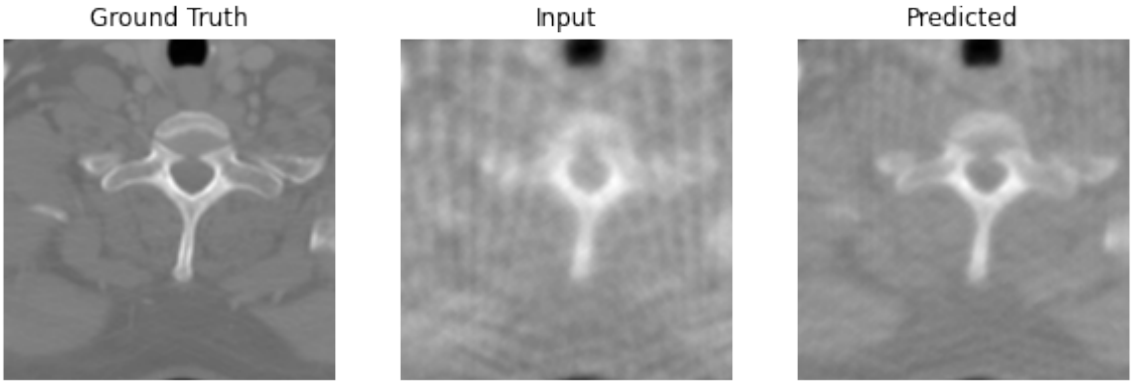

Figure 14: Zoom-In CT image of chest section for downfactor 40

5. Conclusion and Future Work

The impending risk of radiation exposure has driven the research to develop proficient methods of image reconstruction from sparse view CT using regularization methods to

intellectual networks. The procedure put forward in this paper would show that the incorporation of attention gates in the U-Net has positive pay off in CT image reconstruction. With more adaptable projection data and admittance to high processors, the exploration can be taken forward to dig further into the potential outcomes of tuning the profound learning procedures to perfect reconstruction. The time taken by the model can be taken as a boundary for assessment. The venture is expected to be saved open source for future examination.

Acknowledgments

The authors would wish to thank the authorities and staff of the Central Computer Centre (CCC) at the National Institute of Technology Calicut, Kerala, India for providing the GPU computing facility. The authors also would like to express the gratitude to MVR Cancer Center and Research Institute for providing the clinical dataset.

References

Hu Chen, Yi Zhang, Mannudeep Kalra, Feng Lin, Yang Chen, Peixi Liao, Jiliu Zhou, and Ge Wang. Low-dose ct with a residual encoder-decoder convolutional neural network. *IEEE Transactions on Medical Imaging*, 36:2524–2535, 06 2017. doi: 10.1109/TMI.2017.2715284.

Natalie Braun Cynthia H. McCollough, Andrew N. Primak. Strategies for reducing radiation dose in ct. *National Center for Biotechnology Information Public Health Information(PMC)*, March 2017.

K. Mueller G. Wang, J. C. Ye and J. A. Fessler. Image reconstruction is a new frontier of machine learning. *IEEE Transactions on Medical Imaging*, vol. 37, no. 6:289–1296, June 2018.

Yoseop Han, Jaejun Yoo, and Jong Chul Ye. Deep residual learning for compressed sensing ct reconstruction via persistent homology analysis. 11 2016.

Kyong Jin, Michael Mccann, Emmanuel Froustey, and Michael Unser. Deep convolutional neural network for inverse problems in imaging. *IEEE Transactions on Image Processing*, PP, 11 2016. doi: 10.1109/TIP.2017.2713099.

Eunhee Kan, Junhong Min, and Jong Chul Ye. Wavenet: a deep convolutional neural network using directional wavelets for low-dose x-ray ct reconstruction. *Medical Physics*, 44, 10 2016. doi: 10.1002/mp.12344.

James M Kofler Juan C Lifeng YuXin Liu, Shuai Leng and Ramirez-Giraldo. Radiation dose reduction in computed tomography: techniques and future perspective. *National Center for Biotechnology Information, Public Health Information(PMC)*, April 2017.

Jianhua Luo, Jiahai Liu, Wanqing Li, Yuemin Zhu, and Ruiyao Jiang. Image reconstruction from sparse projections using s-transform. *Journal of Mathematical Imaging and Vision*, 43:227–239, 2012.

Thomas Brox Olaf Ronneberger, Philipp Fischer. U-net: Convolutional Networks for Biomedical Image Segmentation. *CoRR*, May 2015.

Olaf Ronneberger, Philipp Fischer, and Thomas Brox. U-net: Convolutional networks for biomedical image segmentation. In Nassir Navab, Joachim Hornegger, William M. Wells, and Alejandro F. Frangi, editors, *Medical Image Computing and Computer-Assisted Intervention – MICCAI 2015*, pages 234–241, Cham, 2015. Springer International Publishing. ISBN 978-3-319-24574-4.

Vinod Todwal Shailendra Tiwari, Deepikanshu Chouksey. Regularization based simultaneous algebraic reconstruction techniques for computed tomography. *IEEE Transactions on Medical Imaging*, March 2017.

Emil Sidky, Chien-Min Kao, and Xiaochuan Pan. Accurate image reconstruction from few-view limited-angle data in divergent-beam ct. 14, 05 2009.

Jiaxi Wang, Jun Liang, Jingye Cheng, Yumeng Guo, and Li Zeng. Deep learning based image reconstruction algorithm for limited-angle translational computed tomography. *PLOS ONE*, 15(1):1–20, 01 2020. doi: 10.1371/journal.pone.0226963. URL https://doi.org/10.1371/journal.pone.0226963.

Izzet Yavuz, Mochamad Rizal, and Bramma Kiswanjaya. The possible usability of three-dimensional cone beam computed dental tomography in dental research. *Journal of Physics: Conference Series*, 884:012041, 08 2017. doi: 10.1088/1742-6596/884/1/012041.